Journal of Physiology and Biochemistry (2023) 79:297–311
https://doi.org/10.1007/s13105-022-00939-9

ORIGINAL ARTICLE

Liraglutide provides cardioprotection through the recovery of mitochondrial dysfunction and oxidative stress in aging hearts

Aysegul Durak[1] · **Belma Turan**[2]

Received: 4 February 2022 / Accepted: 3 December 2022 / Published online: 14 December 2022

Abstract

Glucagon-like peptide-1 receptor (GLP-1R) agonists improve cardiovascular dysfunction via the pleiotropic effects behind their receptor action. However, it is unknown whether they have a cardioprotective action in the hearts of the elderly. Therefore, we examined the effects of GLP-1R agonist liraglutide treatment (LG, 4 weeks) on the systemic parameters of aged rats (24-month-old) compared to those of adult rats (6-month-old) such as electrocardiograms (ECGs) and systolic and diastolic blood pressure (SBP and DBP). At the cellular level, the action potential (AP) parameters, ionic currents, and Ca^{2+} regulation were examined in freshly isolated ventricular cardiomyocytes. The LG treatment of aged rats significantly ameliorated the prolongation of QRS duration and increased both SBP and DBP together with recovery in plasma oxidant and antioxidant statuses. The prolonged AP durations and depolarized membrane potentials of the isolated cardiomyocytes from the aged rats were normalized via recoveries in K^+ channel currents with LG treatment. The alterations in Ca^{2+} regulation including leaky-ryanodine receptors (RyR2) could be also ameliorated via recoveries in Na^+/Ca^{2+} exchanger currents with this treatment. A direct LG treatment of isolated aged rat cardiomyocytes could recover the depolarized mitochondrial membrane potential, the increase in both reactive oxygen and nitrogen species (ROS and RNS), and the cytosolic Na^+ level, although the Na^+ channel currents were not affected by aging. Interestingly, LG treatment of aged rat cardiomyocytes provided a significant inhibition of activated sodium-glucose co-transporter-2 (SGLT2) and recoveries in the depressed insulin receptor substrate 1 (IRS1) and increased protein kinase G (PKG). The recovery in the ratio of phospho-endothelial nitric oxide (pNOS3) level to NOS3 protein level in LG-treated cardiomyocytes implies the involvement of LG-associated inhibition of oxidative stress-induced injury via IRS1-eNOS-PKG pathway in the aging heart. Overall, our data, for the first time, provide important information on the direct cardioprotective effects of GLP-1R agonism with LG in the hearts of aged rats through an examination of recoveries in mitochondrial dysfunction, and both levels of ROS and RNS in left ventricular cardiomyocytes.

Keywords Mitochondria · Intracellular Na^+ · Sodium/glucose-co-transporter · Aging heart

Key points:
GLP-1 provides cardioprotection in aging heart, directly preserving mitochondria function.
It attenuates high ROS and RNS productions via recoveries in mitochondria and cytosolic Na^+ levels via inhibition of ventricular SGLT2.
The benefits of GLP-1 are via inhibition of oxidative stress-induced injury in the IRS1-eNOS-PKG pathway.

✉ Belma Turan
belma.turan@medicine.ankara.edu.tr;
belma.turan@lokmanhekim.edu.tr

[1] Department of Biophysics, Ankara University Faculty of Medicine, Ankara, Turkey

[2] Department of Biophysics, Lokman Hekim University Faculty of Medicine, Ankara, Turkey

Abbreviations

CVDs	Cardiovascular diseases
cGMP	Cyclic guanosine monophosphate
DCFDA	Chloromethyl-2′,7′-dichlorodihydrofluoroscein diacetate
ECGs	Electrocardiograms
NOS3	Endothelial NOS, also known as nitric oxide synthase 3
GLP-1R	Glucagon-like peptide-1 receptor
GLUT4	Glucose transporter type 4
IRS1	Insulin receptor substrate 1
LG	Liraglutide
MetS	Metabolic syndrome
MMP	Mitochondrial membrane potentials
NCX	Na^+/Ca^{2+} exchanger
PKG	Protein kinase G

ROS	Reactive oxygen species
RNS	Reactive nitrogen species
RyR2	Cardiac ryanodine receptors
SGLT2	Sodium-glucose co-transporter 2
SR	Sarcoplasmic reticulum
TOS	Total oxidant status
TAS	Total antioxidant status

Introduction

Mammalian aging is a physiological process, associated with changes that gradually increase, which lead further to important insufficiencies in various organ functions due to their negative affects. Therefore, aging is a dominant risk factor for cardiovascular diseases (CVDs), including structural and functional remodeling in the heart, which are leading causes of human death, worldwide [18]. International consensus via experimental and clinical studies is that there exists an correlation between aging, CVDs (at most, via the development of left ventricular hypertrophy in the heart), and cardiometabolic disturbances, including insulin resistance [18, 33]. Cardiac aging is also an intrinsic process accompanied by molecular and cellular changes. Both clinical and experimental data point out that cardiac aging is mainly characterized by a prolonged QT interval on the surface electrocardiograms (ECGs), including a reduction in the maximum heart rate, and a significant decrease in the contractile activity due to cardiometabolic disturbances [18].

Moreover, various studies have shown impairment in cellular redox status, metabolic flexibility, and organelle dynamics in aged hearts [21]. Some clinical observations demonstrated parallelism between the marked functional decline in the heart and the induction of insulin resistance, although focusing on subjects with a normal blood glucose level and body weight [7]. Most experimental studies support this subject-related insulin resistance and cardiometabolic disturbances which are factors that further underline the impairment of electrophysiological activities of cardiomyocytes [5, 29]. Correspondingly, experimental animal studies further support these statements with findings associated with either cardiac-specific insulin receptor deletion or insulin application to animals [30].

Aging is associated with a decline in physiological function leading to various chronic diseases including diabetes, which is also accepted as the cause of accelerated aging, being linked to many abnormalities in metabolic regulation. Aging adversely affects not only hormonal secretions but also their biological availability, while the commonly observed age-related changes among them are in insulin sensitivity [31]. Studies have documented a relationship between circulating concentrations of the incretin hormone, glucagon-like peptide-1 (GLP-1), and insulin responses in obese and metabolic syndrome (MetS) individuals [25]. Accordingly, recent studies have also shown an excellent cardioprotective effect amoung GLP-1 receptor (GLP-1R) agonists, through their action in regards to the stimulation of insulin secretion and the reduction of glycated hemoglobin levels not only in diabetics but also in nondiabetics without important side effects [22]. Furthermore, we, previously, have demonstrated that treatment of GLP-1R agonist liraglutide (LG) among rats with MetS significantly ameliorated long their QT interval, through pleiotropic effects, such as the alleviation of electrical abnormalities, Ca^{2+} homeostasis, and mitochondrial dysfunction together with depressed ATP production in ventricular cardiomyocytes. Similar to our previous study, others have demonstrated that the promotion of the mitochondrial metabolism in vascular smooth muscle cells with GLP-1 can be achieved via the enhancement of endoplasmic reticulum-mitochondria couplings [24]. Furthermore, both experimental and clinical data have also demonstrated that the amelioration of both oxidative and nitrosative stress (ROS and RNS) in hyperglycemic and hyperinsulinemic conditions is possible with GLP-1R agonism [2, 10]. More interestingly, recent studies focused on the cardioprotective effects of GLP-1R agonism through its direct effect on mitochondria, oxidative stress, and ventricular excitability in cells responding to various pathological stimuli [1, 17]. Although the molecular biology of GLP-1 and the presence of GLP-1Rs are known in mammalian ventricular cardiomyocytes, mixed results have been reported, and, therefore, the effects of this peptide in the intact ventricular myocardium of individuals without hyperglycemia have not yet been made clear.

In previous studies, we, as well as others, have mentioned a possible connection between insulin resistance in aged mammalians and severe heart dysfunction [3, 29, 32, 33]. In our previous studies, we demonstrated the existence of the sodium-glucose co-transporter 2 (SGLT2) in rat left ventricular cardiomyocytes by measuring the rats' mRNA level and then its activation in insulin-resistant MetS rat cardiomyocytes and its recovery with an SGLT2 inhibitor [11]. In another study, we further demonstrated its activated mRNA and protein expression levels in aged rat ventricular cardiomyocytes [28]. Indeed, both clinical and experimental studies have described the benefits of in vitro and in vivo SGLT2-selective inhibitors for diabetic mammalians [14, 36]. The beneficial effects of SGLT2 inhibitors include the recovery effects in regards to the electrical activities of cardiomyocytes; the alteration in intracellular Ca^{2+}, Na^{+}, and H^{+} regulations; mitochondrial dysfunction; and the control of the systemic and cellular redox status of mammalians with insulin resistance. However, the mechanisms of SGLT2 inhibition that improve cardiovascular outcomes are not fully understood.

Taking our previous studies with aged rats into consideration, as well as all of the above relationships between GLP-1R status and insulin resistance, increased stress stimuli, and depressed mitochondrial dysfunction in aging mammalians, here, we intended to examine some mechanistic studies with animals (in vivo) and in vitro investigations in isolated ventricular cardiomyocytes to better understand whether GLP-1R agonist LG has a direct effect on aging heart function. Furthermore,as we, previously, demonstrated significantly high levels of reactive oxygen and nitrogen species (ROS and RNS) in the isolated left ventricular cardiomyocytes from either MetS or aged rats with significant oxidation in protein thiols [11], we now wanted to examine whether GLP-1R agonism can present an antioxidant-like action in aged rats. Moreover, as we have demonstrated the important contribution of activated SGLT2 on heart dysfunction from either aged or MetS rats and the important benefits of SGLT2 inhibitors on these cardiac dysfunctions [11, 29], we also intended this time to assess whether a GLP-1R agonist can ameliorate the activation of the cardiac SGLT2 in the aging heart.

Materials and methods

Ethics statement

In this study, experiments with animals were performed following the guide for the Management and Use of Laboratory Animals issued by the National Institutes of Health and approved by the Institutional Animal Care and Use Committee at Ankara University, Ankara (No. 2016–18-165).

Experimental animals

Male Wistar rats were used at the age of 24 months (Aged group; $n = 10$) and 6 months (Con group; $n = 9$). All rats were given free access to tap water and exposed to a 12-h light–dark cycle. All animals were housed in standard rat cages, 2–3 per cage, and were fed a standard chow ad libitum daily. For in vivo treatments with a GLP-1R agonist LG, we followed previous studies. We used different doses and different experimental periods for the in vivo treatment in different types of animal species. The authors used an LG treatment with 200 µg/kg/day for 6 weeks, and following 41 weeks, they observed significant effects on hyperglycemia and insulin level in older Zucker diabetic fatty (ZDF) rats with insulin resistance in comparison to those of younger rats [6, 16, 20]. In our previous study, we treated adult MetS rats with LG (300 µg/kg/day) for 4 weeks and found significant recoveries in heart function [10]. Therefore, we treated aged rats with 300 µg/kg/day LG for 4 weeks (intraperitoneal administration; Aged + LG group; $n = 10$) while the second group of aged rats and adult rats received the vehicle for the same period. Following fasting overnight with free access to tap water, the measurement of both body weights, blood glucose levels, and insulin resistance among all the rats was carried out, as described previously [11]. The HOMA index was measured as described elsewhere [11, 23, 34, 35] and used the following equation for calculation: HOMA index (IR): [fasting insulin (µU/mL) × fasting glucose (mmol/L)] / 22.5.

Plasma parameters

Plasma TNF-α and IL-6 levels were determined using a commercially available Thermo Fisher (Thermo Fisher Scientific Co., USA) ELISA kit following the manufacturer's instructions. The TNF-α and IL-6 results were presented as ng/L.

Plasma total antioxidant status (TAS) and total oxidant status (TOS) levels were measured with a spectrophotometer (microplate reader; Synergy H1) using commercially available kits (Rel Assay Diagnostics, Gaziantep, Turkey). The results were expressed as mmol Trolox Eqv/L for TAS and µmol H_2O_2 Eqv/L for TOS.

Surface electrocardiogram recordings

Following the experimental period, the in situ surface ECGs of all rats were recorded for 10 min under mild anesthesia before their scarification was determined by using two electrodes placed on forepaws with a third one on the tail as a reference electrode (MP150, BIOPAC Systems, Inc., USA), as described previously [11]. The parameters such as QRS duration, RR interval, and ST interval were analyzed from surface-recorded ECGs. The systolic and diastolic blood pressures (SBP and DBP) were measured by an indirect tail-cuff method via a NIBP200-A non-invasive blood pressure meter (MP150, BIOPAC Systems Inc., USA).

Cardiomyocyte isolation

Left ventricular cardiomyocytes were freshly isolated by using the enzymatic method, as described elsewhere [11]. Hearts were removed from the rats under mild anesthesia (30 mg/kg sodium pentobarbital), then perfused at 37 °C with a Ca^{2+}-free HEPES-buffered solution. Following 5 min of perfusion of the hearts, a fresh buffer supplemented with 1.2 mg/mL collagenase (Worthington collagenase type 2, USA) was recirculated for 30–40 min with a speed of 8 mL/min. Following the collagenase perfusion, the ventricles were cut off and stirred slowly into the Ca^{2+}-free medium to disperse the myocytes. The cells were then suspended at 37 °C in the HEPES-buffered solution while the Ca^{2+} level was increased in a graded manner to a concentration of

physiological level. The isolated cardiomyocytes were kept in the HEPES-buffered solution, containing BSA at 37 °C. The yield level of well-elongated isolated cells was about 70–80% following exposure to relatively low Ca^{2+} (1 mM).

To determine the in vitro effects of LG, most studies were performed in cultured cells through the incubation of cells with different concentrations of LG ranging between 100 nM and 10 μM for several hours [12, 15, 19]. Following previous studies, we incubated the aged rat cardiomyocytes with LG at either 1 nM, 10 nM, or 100 nM for 3–4 h; however, there were fewer changes in the parameters of the cardiomyocytes such as mitochondrial membrane potential (MMP) and ROS level with 1 nM or 10 nM LG treatment than that of the 100 nM treatment, although the liability of the cells was similar. Therefore, we used only 100 nM LG-treated cardiomyocytes for all in vitro investigations.

Electrophysiological investigations in the isolated cardiomyocytes

All electrical parameters in the isolated cardiomyocytes were determined using an Axoclamp patch-clamp amplifier either in current-clamp or voltage-clamp mode at room temperature (23 ± 2 °C). The recordings were sampled and digitized at 5 kHz using an analog-to-digital converter and software (Axopatch 200B amplifier and Digidata 1200A and pCLAMP 10.0; Axon Instruments, USA).

Action potential recordings were performed in the newly isolated ventricular cardiomyocytes using glass electrodes with an access resistance of 1.5–2.5 MΩ, as described previously [11]. The parameters such as their maximum amplitudes and repolarization times were determined as percentage changes at 25, 50, 75, and 90 time points ($APD_{25, 50, 75, 90}$) and were calculated from the original action potential traces.

Voltage-dependent K^+ channel current (I_K) recordings were performed using 1.5–2.5 MΩ patch electrodes in a whole-cell voltage clamping configuration, as described previously [11]. Keeping the membrane potentials of cells at − 70 mV and after clamping the cells and applying a pre-pulse protocol (to block Na^+ channels), electrical stimulations with 500-ms pulses were applied 20 times at 5-s intervals to the cells under the application of Co^{2+} to block Ca^{2+} channels.

The recording of the L-type Ca^{2+} currents (I_{CaL}) was performed as described previously. Avoltage clamp protocol was used to record I_{CaL} that included a pre-pulse from − 70 to − 55 mV (to inactivate the Na^+ channel currents) followed by 300-ms depolarizing voltage steps between − 60 and + 80 mV.

The TTX-sensitive Na^+ channel currents (I_{Na}) were determined at room temperature, as described, previously [11]. A pre-pulse protocol (holding potential at − 80 mV) was used to record these currents, and it calculated a difference between the negative peak and the current obtained at the end of the pulse.

Na^+/Ca^{2+} exchanger (NCX) currents (I_{NCX}) were performed as described previously [10]. I_{NCX} was recorded with glass electrodes containing an internal solution (in mM) of CsCl 65, $CaCl_2$ 10.92, EGTA 20, HEPES 10, MgATP 5, $MgCl_2$ 0.5, and TEA-Cl 20 at pH 7.2. The extracellular bathing solution was contained in mM: NaCl 130, TEA-Cl 10, Na-HEPES 11.8, $MgCl_2$ 0.5, $CaCl_2$ 1.8, ryanodine 0.005, nifedipine and 0.02, glucose 10 at pH 7.4. Both inward and outward parts of I_{NCX} were obtained from a protocol composed of a descending ramp from + 80 to − 120 mV at 0.1 mV/ms with a holding potential of − 40 mV.

Every current value (pA) for every depolarizing potential was divided by its membrane capacitance (pF) for the presentation of the current density. The current–voltage relations of the channels (I-V curves) were calculated from online current recordings. Voltage-clamp and current-clamp experimental protocols were controlled with the Clampex program, and all online recording signals were analyzed using the Clampfit program of the pClamp 10.2 software (Molecular Devices, San Jose CA, USA).

The determination of parameters associated with Ca^{2+} regulation in the isolated cardiomyocytes

The newly isolated cardiomyocytes were incubated with Fura-2 AM (4 μM for 45 min) at room temperature (23 ± 2 °C) in Tyrode's solution, as described elsewhere [11]. The basal level of free Ca^{2+} ($[Ca^{2+}]_i$) and also the transient changes of $[Ca^{2+}]_i$ under electric field stimulation in the cardiomyocytes were monitored by applying a 25-V square pulse, and stimulating the 0.2-Hz frequency (10 ms). The changes in the fluorescence intensities were detected using the microspectrofluometer and FELIX software (Photon Technology International, Inc., NJ, USA) with an emission of 520 nm at wavelengths of 340/380 nm. The fluorescence ratio (difference between basal and peak $F_{340/380}$) was used as an indicator of intracellular free Ca^{2+} changes in each cell.

Sarcoplasmic reticulum (SR) leakage was measured online in the presence of tetracaine, as described previously [27]. Briefly, following the monitoring of the basal level of cytosolic Ca^{2+} in resting cardiomyocytes, the SR load was determined by an SR Ca^{2+} pump-mediated Ca^{2+} reuptake in the cardiomyocytes. Following electric field stimulation, Fura-2 AM-loaded cells were perfused with a special solution (contained as 0 Na^+/0 Ca^{2+}, by replacing NaCl and $CaCl_2$ with equimolar NMDG or 10 mmol/L EGTA, respectively). Then, the loaded cells were stimulated with 10 mmol/L caffeine for 1 s to induce full Ca^{2+} release from SR. Then, the level of intracellular Ca^{2+}, measured in the

presence of tetracaine, could provide the Ca^{2+} leak based on the ryanodine receptors and the SR Ca^{2+} content.

The determination of mitochondrial functions

The MMP levels were obtained by using confocal microscopy (Leica TCS SP5) in newly isolated left ventricular cardiomyocytes loaded with a voltage-sensitive fluorescence dye JC-1 (with 4 μM for 30-min incubation). The cells flowing the loading procedure were excited at 488 nm, and the red fluorescent image was detected at both 535 nm and 585 nm. Then, they were calibrated with carbonylcyanide 4-(trifluoromethoxy)phenylhydrazone, FCCP (5 μM with acute application) to determine the fluorescence intensity changes.

The cellular levels of ROS production in newly isolated cardiomyocytes were measured as responses to acute H_2O_2 (100 μM) exposure, as described elsewhere [11]. Cells were loaded with a ROS indicator chloromethyl-2′,7′-dichlorodihydrofluoroscein diacetate (DCFDA, 10 μM for 60-min incubation) and then examined with a laser scanning microscope (Leica TCS SP5, Germany). The DCFDA-loaded cells were excited at 488 nm, and emissions were collected at 560 nm. To prevent photobleaching and cell damage, the laser line was kept at 4–6% of maximal intensity. To obtain a maximal fluorescence intensity as associated with ROS production, cells were exposed to a HEPES-buffered solution supplemented with H_2O_2 (100 μM). The peak fluorescence changes ($\Delta F/F0$, where $\Delta F = F - F_0$; F identified as local maximum elevation of fluorescence intensity over basal level, F_0) were calculated from confocal images, and the results were given as percentage changes in the fluorescence intensities.

The cellular levels of RNS production in freshly isolated cardiomyocytes were determined in an RNS indicator DAF-FM loading of the cells (5 μM for 60-min incubation) by using a laser scanning microscope (Leica TCS SP5, Germany), as described previously [11]. The DAF-FM-loaded cells were excited at 488 nm, and emissions were collected at 520 nm. To maximize the level of NO, cells were superfused with ZipNONO (100 μM) supplemented with a HEPES-buffered solution. The data are presented as comparisons of fluorescence intensity changes as percentage changes among these three groups.

The determination of thet cellular free Na^+ level using confocal microscopy

The cellular basal level of Na^+ ($[Na^+]_i$) was determined in Na^+-specific fluorescence dye (SBFI)-loaded cardiomyocytes using confocal microscopy (Leica TCS SP5, Germany), as described previously [11]. To determine the fluorescence changes for $[Na^+]_i$, the loaded cells were excited at 350 nm/380 nm and their emissions were collected at 510 nm. The background fluorescence measured from a cell-free field was subtracted from all recordings before the calculation of fluorescence ratios. All fluorescence changes are used to present the levels of the related parameter in the manuscript.

Histological examination

The morphological examination was performed using semi-thin sections from freshly isolated ventricular cardiomyocytes, and araldite blocks were prepared using examination methods for TEM as previously described [4]. Semi-thin sections of 1-mm thickness were taken from the blocks using a Leica Ultracut R ultramicrotome (Leica, Solms, Germany). The sections were dried. They were kept in distilled water with toluidine blue-Azur II dye containing 1% borax, 1% toluidine blue, and 1% Azur II in a heater at 50°–60 °C until the paint dried. They were washed with distilled water and dried. They were then cleared with xylene and covered with entellan. The stained preparations were examined with an Axio Scope A1 (Carl Zeiss, Germany) microscope and photographed. The surface areas of the cardiomyocytes were analyzed (Axio-Vision software) by two independent blinded investigators for morphology at about 100 cells for each group. The relative densities from the samples were determined for the mountant, and the same arbitrary density units were used in all evaluations.

Western blotting analysis

Western blotting experiments were performed in the isolated cardiomyocytes, as described elsewhere [11]. The isolated cells were first homogenized, and then, the supernatant was centrifuged at $10{,}000 \times g$ for 15 min. Following this, the protein concentration was determined using the Bradford method. Following classical procedures, the membranes were incubated with bovine serum albumin for 3 h and then incubated with primary antibodies of SGLT2 (ab37296, 1:1000), PKG (sc-8170 1:200; Santa Cruz), IRS1 (sc-8038 1:400; Santa Cruz), GLUT4 (sc-1607 1:400; Santa Cruz), NOS3 (Santa Cruz, sc-654, 1:250), and pNOS3 (Ser1177; Santa Cruz, sc-12972, 1:250) in BSA (3%). GAPDH (sc-365062 1:1000; Santa Cruz) and β-actin (Santa Cruz, sc-47778, 1:5000) were used for reference proteins. ImageJ software was used to determine band density associated with the investigated proteins.

Statistical analysis

We used GraphPad Prism 6.0 (GraphPad Software, Inc, La Jolla, CA) to process the data. All data are expressed as mean ± SEM, and the mean differences among groups were

compared by either one-way ANOVA or Student's *t* test at a 0.05 level of significance.

Results

The impact of LG treatment on the systemic parameters of aged rats

We first determined the parameters of LG-treated aged rats in comparison with either untreated aged rats or adult rats. The systemic parameters of all groups are presented in Table 1. There were no significant differences between the mean body weights of the aged rats and LG-treated aged rats compared to the adult rats following the 4-week treatment period. Similarly, the final fasting blood glucose levels of the treated or untreated aged rats are not significantly different from the adult rats. The HOMA indexes were not significantly different among either the LG treated or untreated aged rats, while the HOMA indexes of them were also not significantly different from the adult rats.

To demonstrate the systemic anti-inflammatory effects of LG treatment in aged rats, we determined the plasma levels of TNF-α and IL-6. As can be seen in Table 1, neither plasma TNF-α level nor plasma IL-6 level is significantly different in the aged rats in comparison to the adult rats. Also, the treatment of aged rats with LG for 4 weeks could not significantly affect these parameters. Furthermore, to demonstrate the possible antioxidant-like effects of LG treatment in aged rats, we determined the plasma TOS and TAS levels as presented in Table 1. The TOS level was significantly high in the aged rats in comparison to those of adults, and the treatment of aged rats with LG for 4 weeks could induce significant recovery in this parameter. Furthermore, although the plasma TAS level was slightly (but not significantly) low in the aged rats in comparison to those of adults, the treatment of aged rats with LG for 4 weeks could induce a significant increase in this parameter.

The levels of SBP and DBP were found to be significantly high in the aged rats compared to the adult rat group, while these values were normalized with an LG administration to the aged rats (Table 1). We also determined the effect of systemic LG administration on the parameters of surface ECGs. The systemic administration of LG ameliorated significantly the prolonged QRS duration with slight but not significant effects on the RR interval and the ST interval in the aged rats (Table 1).

The LG treatment of the aged rats ameliorated the abnormal electrical activities of ventricular cardiomyocytes

The representative AP traces measured in freshly isolated ventricular cardiomyocytes are given in Fig. 1A. The mean (± SEM) values of all time points of AP repolarization phases such as APD_{25}, APD_{50}, APD_{75}, and APD_{90} are given in Fig. 1B. As can be seen in Fig. 1B, a systemic administration of LG induced significant decreases in the prolonged AP duration at all time points of repolarization phases. We also determined a significant effect on the depolarized resting membrane potential with no significant effect on the maximum amplitudes of APs (Fig. 1C, D, respectively). Figure 1E demonstrates the significant amelioration in the depressed I_K in terms of their maximum amplitudes determined at + 70 mV (right) and I-V characteristics (left).

We also examined the statuses of I_{CaL} and I_{Na} in the ventricular cardiomyocytes from the aged rats. As can be seen in Fig. 2A, the maximum amplitudes of the I_{CaL} determined

Table 1 Systemic parameters of rats determined after the experimental period

Groups/parameters	Control group ($n=9$)	Aged group ($n=10$)	Aged + LG group ($n=10$)
Body weights (g)	327 ± 31	316 ± 29	300 ± 33
Blood glucose (mg/dL)	76.3 ± 5.4	85.5 ± 9.3*	78.9 ± 8.4†
HOMA index	9.8 ± 4.3	13.1 ± 6.6*	11.9 ± 5.5
Systolic blood pressure (mmHg)	125.3 ± 7.1	167.1 ± 9.1*	116.3 ± 5.3†
Diastolic blood pressure (mmHg)	96.1 ± 5.9	120 ± 6.1*	83 ± 8.2†
QRS duration (s)	0.064 ± 0.002	0.088 ± 0.01*	0.075 ± 0.001†
RR interval (s)	0.199 ± 0.02	0.271 ± 0.03*	0.254 ± 0.10*
ST interval (s)	0.013 ± 0.0007	0.015 ± 0.0007*	0.014 ± 0.0019*
Plasma IL-6 (ng/L)	13.59 ± 0.47	15.08 ± 0.65	13.00 ± 0.86
Plasma TNF-α (ng/L)	3.7 ± 0.60	3.5 ± 0.48	3.6 ± 0.46
Plasma TOS (μM H_2O_2)	8.3 ± 0.83	17.45 ± 1.75*	14.30 ± 2.6†
Plasma TAS (mM Trolox)	0.92 ± 0.09	0.89 ± 0.10	1.33 ± 0.17†

The experimental animals are grouped as control group (Con group; 6-month-old rat), aged group (Aged group; 24-month-old rats), and LG-treated aged group (Aged + LG group rats; 300 μg/kg/day for 4 weeks). All values are presented as mean (± SEM), and *n* represents the numbers of rats. Significance levels at $^{*}p<0.05$ *vs*. Con group and $^{\dagger}p<0.05$ *vs*. Aged group

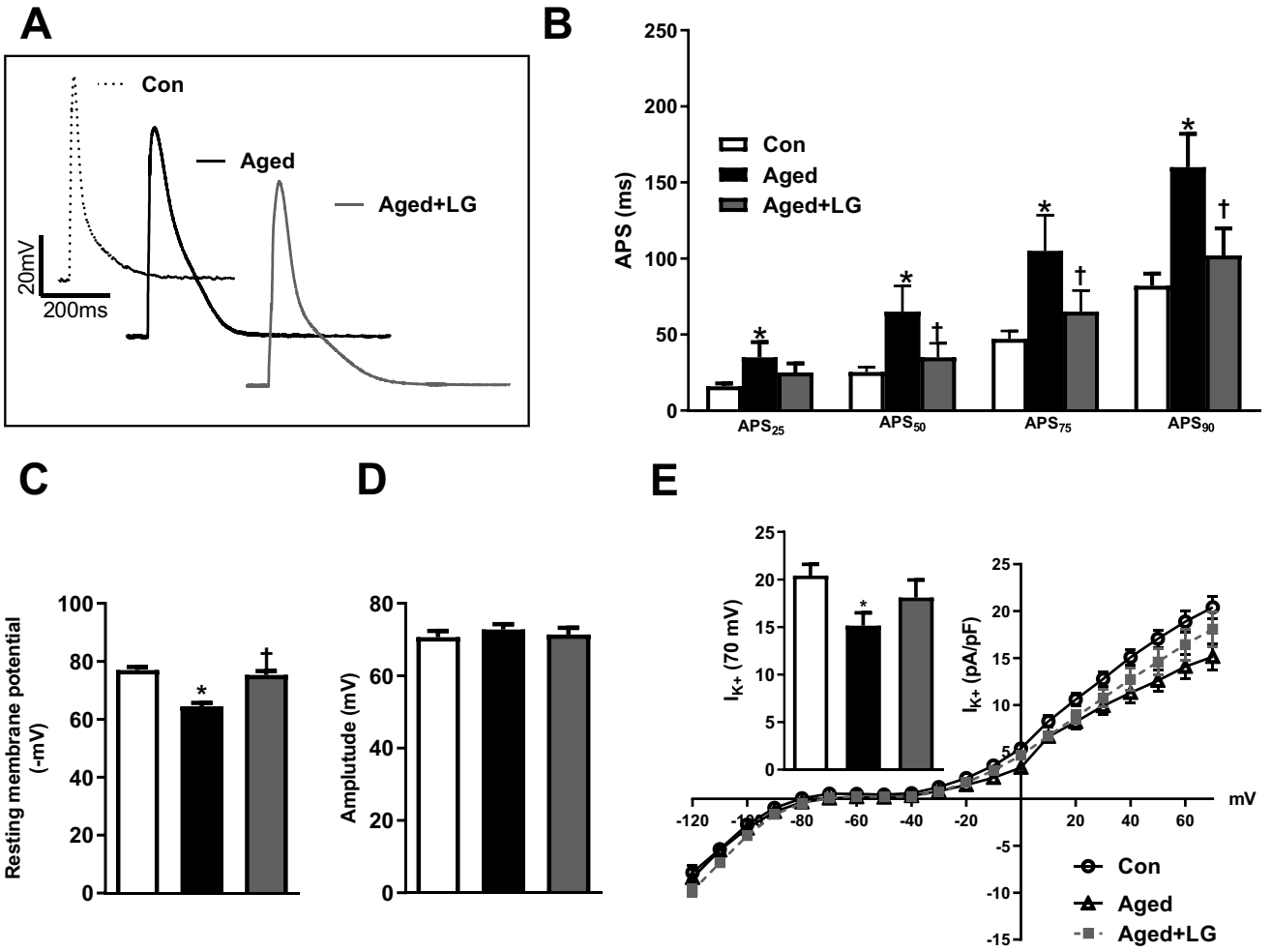

Fig. 1 The effects of LG treatment on parameters of AP and I_K in freshly isolated ventricular cardiomyocytes from aged rats. **A** Representative original action potential recordings in the ventricular cardiomyocytes isolated from rat hearts in the adult rats (Con group), the aged rats (Aged group), and LG-treated (300 μg/kg/day for 4 weeks) aged rats (Aged + LG group). **B** The repolarization phases of APs (APD_{25}, APD_{50}, APD_{75}, APD_{90}). **C** The maximum amplitudes of APs. **D** The resting membrane potentials of the cells. **E** The I-V characteristics of the I_K at − 120 mV (maximum inward) and + 70 mV (maximum outward) stimulation potentials (right). The maximum values of I_K measured at + 70-mV stimulation potential as bar graphs (left). All values in bar graphs are presented as a mean (± SEM) from at least 25–30 recordings from 15 to 20 cells/group isolated from 6–7 rats per group. For a proper comparison of the currents among these three groups, all types of current recordings were calculated as current densities by dividing every current value by the cell capacitance (represented as pA/pF). The significance levels are at $^{*}p < 0.05$ vs. Con group and $^{\dagger}p < 0.05$ *vs.* Aged group

at 0 mV are not significantly different among all groups (inset), and no differences in their I-V characteristics. As can be given in Fig. 2B, the maximum amplitudes of the I_{Na} determined at − 45 mV are also not significantly different among these three groups (inset). However, there is a right shift in the voltage dependency of these Na^+ channels in the cardiomyocytes from LG-treated aged rats.

In another group of examinations, we determined the I_{NCX} in both forward and reversed directions in the ventricular cardiomyocytes. As can be seen in Fig. 2C, I_{NCX}, in both directions, were found to be significantly increased in the aged rats compared to the adult rats, while they were almost fully normalized with LG treatment of the aged rats (inset). The I-V relations of I_{NCX} for the three groups of rats are given on the left side of the bar graphs in the same figure.

The LG treatment of aged rats recovered alterations in the Ca^{2+} regulation of ventricular cardiomyocytes

We first determined the basal $[Ca^{2+}]_i$ in Fura-2 AM-loaded ventricular cardiomyocytes from the aged rats compared to the adult rat group ratiometrically. As can be seen in Fig. 3A, the basal $[Ca^{2+}]_i$ increased significantly in the aged rats, while this increase was found to be normalized in the LG-treated aged rats. We also examined the intracellular transient releases of Ca^{2+} from SR under electrical stimulation

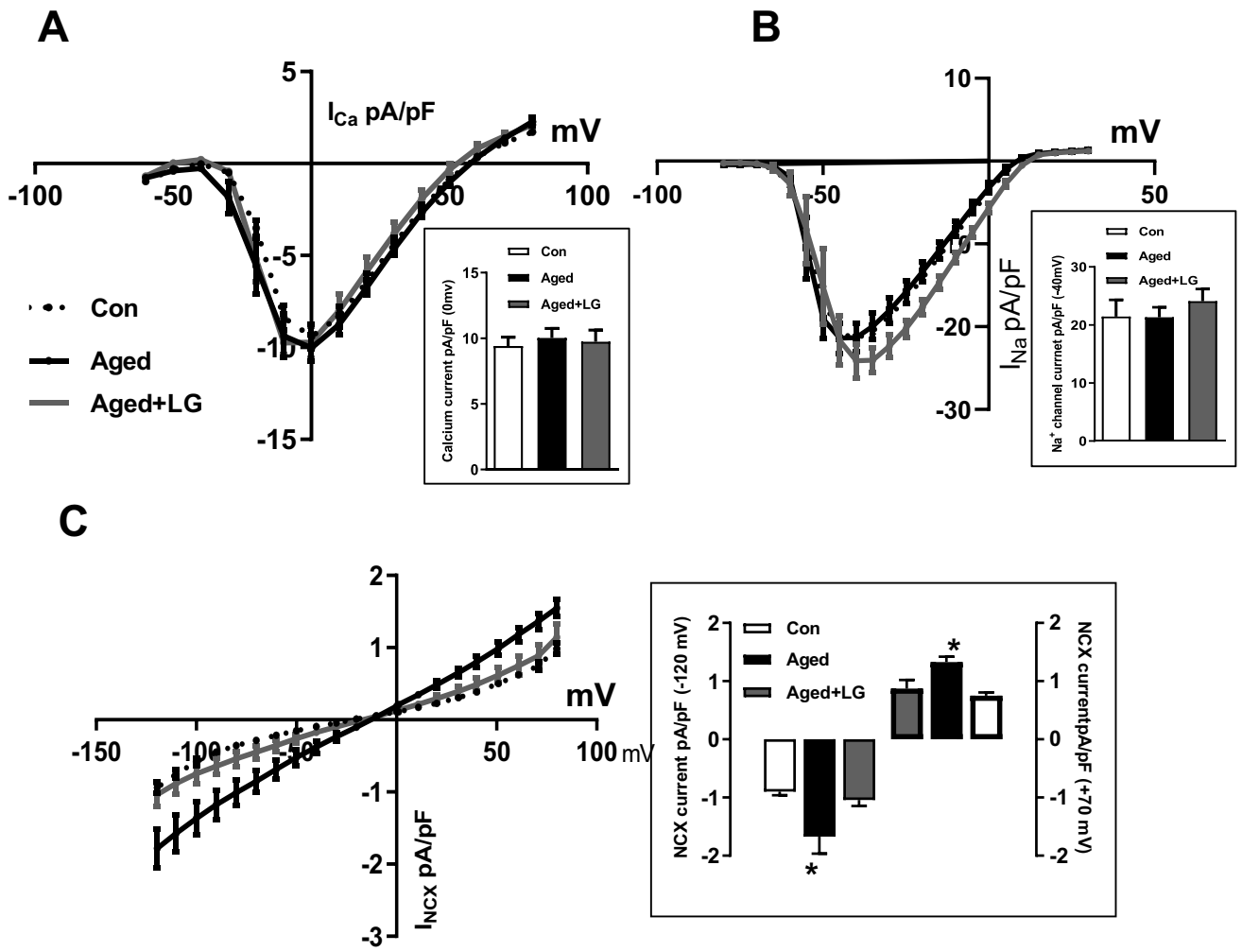

Fig. 2 The effects of LG treatment on ionic currents in the ventricular cardiomyocytes from aged rats. **A** The I-V characteristics of the I_{CaL} (left), and their maximum amplitudes measured at 0 mV (inset). **B** The I-V characteristics of the I_{Na} obtained by applying voltage steps (left), and their maximum amplitudes at − 40 mV (inset). **C** The I-V characteristics of the I_{NCX} obtained from the ramp descending between + 80 mV and − 120 mV. The maximum responses at positive potentials were obtained for I_{NCX} at + 80 mV (inset) and maximum responses at negative potentials for I_{NCX} at − 120 mV. For a proper comparison of the currents among the groups, all types of current recordings were calculated as current densities by dividing every current value by the cell capacitance (represented as pA/pF). All electrophysiological studies were performed with 15–20 cells/group isolated from 6 to 7 rats per group. The bar graphs are representing the mean (± SEM) values of the groups. The ignificance level was at $*p < 0.05$ *vs.* Con group

($[Ca^{2+}]_i$ transients). As can be seen in Fig. 3B, C, the maximum amplitudes of $[Ca^{2+}]_i$ transients were significantly smaller in the aged rats than in the adult rats with prolonged time courses (Fig. 3D), whereas these alterations were found to be fully ameliorated in the LG-treated aged rats.

In the last part of these group examinations, we determined the Ca^{2+} release using an application of SR under tetracaine. As is given in Fig. 3E, the calculated SR Ca^{2+} leak was significantly high among the aged rats compared to the adult rats (right), while the caffeine responses were found to be similar among these three groups (left). In addition, the LG treatment of the aged rats could ameliorate the abnormal SR Ca^{2+} leak significantly.

LG can provide benefits to ventricular cardiomyocytes from aged rats targeting mitochondria

Figure 4A (left) shows the original representative cardiomyocytes loaded with the fluorescent dye JC1 to imagine the fluorescence intensity associated with the MMP of the cells. The fluorescence intensity-level analysis demonstrated that MMP was significantly depolarized in the aged rat cardiomyocytes in comparison to the adult ones, while there was a slight but significant recovery in the LG-incubated (100 nM for 3–4 h) aged cells (Fig. 4A, right).

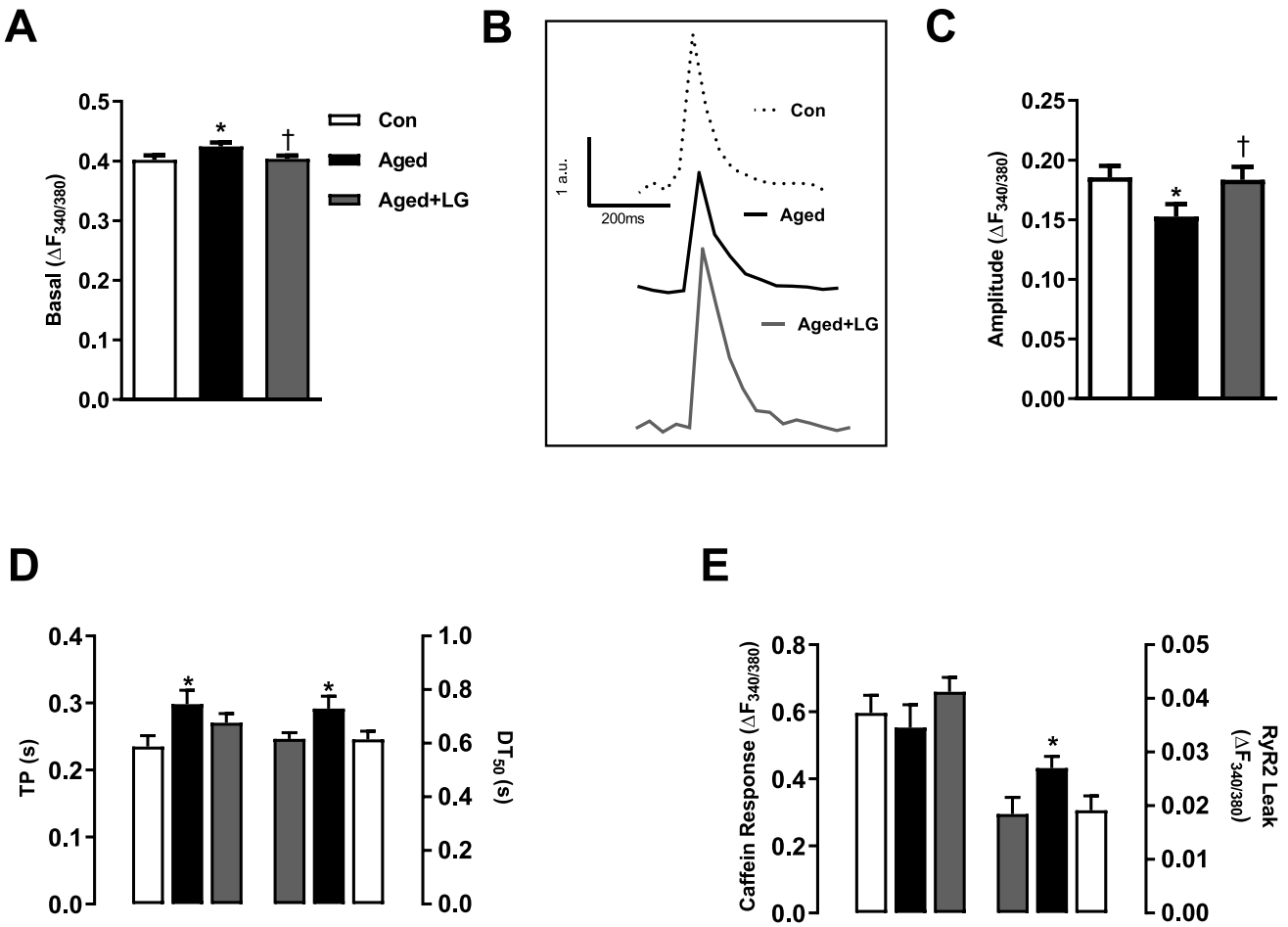

Fig. 3 The LG treatment of aged rats recovered alterations in Ca^{2+} regulation of ventricular cardiomyocytes. **A** The basal resting $[Ca^{2+}]_i$ determined in Fura-2 AM-loaded ventricular cardiomyocytes isolated from rats as the ratio of fluorescence intensity changes. **B** The representative original cellular transient $[Ca^{2+}]_i$ changes under electrical stimulation. **C** The maximum amplitudes of $[Ca^{2+}]_i$. **D** The time courses measured as the time to peak of the transient fluorescence changes (TP, left) and the half-time for recovery of these transients (DT_{50}, right). **E** The calculated level of the Ca^{2+} release as caffeine response (10 mM) (left) and the SR RyR2 leak (right). All data are presented as mean (±SEM) from at least 25–30 recordings from 15 to 20 cells/group isolated from 6 to 7 rats per group. $^{*}p<0.05$ *vs.* Con group and $^{\dagger}p<0.05$ *vs.* Aged group

We also examined the production of cellular ROS by using DCDFA-loaded aged rat cardiomyocytes with or without LG incubation. As can be seen in Fig. 4B (right), the ROS production level was significantly higher in the aged rat cardiomyocytes than in those of the controls. The LG incubation of the aged rat cardiomyocytes could provide a full amelioration in the production of ROS. The representative loaded cell images for the determination of ROS production are given on the left of this figure.

In the last part of this group examination, to examine the role of the cellular level of RNS production in the ventricular cardiomyocytes from the aged rats and the direct effect of LG on these cardiomyocytes, we determined the RNS levels in the DAF-FM-loaded cells as percentage changes in fluorescence intensity responses. As can be seen in Fig. 4C, the RNS level was about 1.5-fold high in the aged rats' group compared to the control group. This high level could be recovered significantly by an LG incubation (100 nM for 3–4-h incubation) of these aged group cardiomyocytes. The representative loaded cell images for the determination of RNS production are given to the left of this figure.

LG can provide a direct benefit to the structure of ventricular cardiomyocytes

To test further a direct cardioprotective effect of LG on the aged rat ventricular cardiomyocytes, we examined them histologically with and without the LG incubation of the ventricular cardiomyocytes (100 nM for 3–4 h) using their semi-thin sections. As can be seen in Fig. 4D, there were marked dilations in the location of T tubules and SR junctions in the ventricular cardiomyocytes from the aged rats (b), representing the loss of

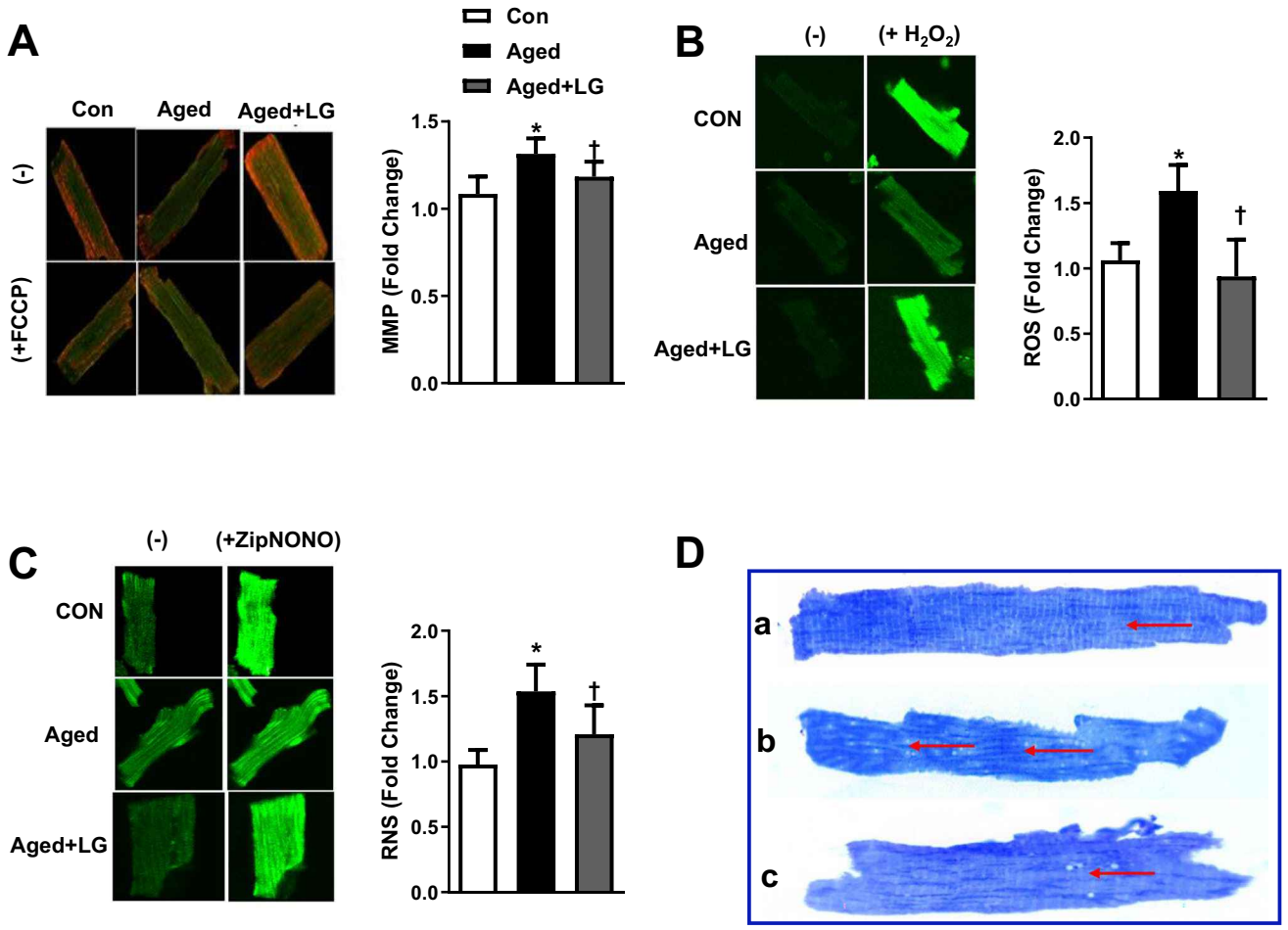

Fig. 4 LG can provide benefits to ventricular cardiomyocytes from aged rats targeting mitochondria and affecting the structure of cardiomyocytes. **A** The mitochondrial membrane potential, MMP, was measured in the ventricular cardiomyocytes loaded with JC-1 from either LG-treated (100 nM for 3–4-h incubation) (Aged + LG) or untreated aged rats (Aged group) compared to those adults (Con group), by using a confocal microscope as the ratio of fluorescence intensity changes. The representative original loaded cells in the left of this figure. **B** The calculated fluorescence intensity changes to present the production of ROS level in the ventricular cardiomyocytes loaded with an oxidant-sensitive fluorescence dye DCDFA and imagined with confocal microscopy. Maximal fluorescence intensity was achieved by a HEPES-buffered solution supplemented with H_2O_2 (100 μM) (right). The representative original loaded cells in the left of the figure. **C** The cellular RNS levels imagined with confocal microscopy in the ventricular cardiomyocytes loaded with a fluorescence dye, DAF. Maximal fluorescence intensity was achieved by a HEPES-buffered solution supplemented with NO donor ZipNONO (100 μM). The representative original loaded cells in the left of the figure. **D** A light microscopy investigation of semi-thin sections from the ventricular cardiomyocytes. The red arrows represent dilatations noted in the regions of the T tubule and SR junction. The cells were dyed toluidine blue, and the magnification was × 100. The data were from at least 25–30 recordings from 15 to 20 cells/group isolated from 5 to 6 rats per group. The bar graphs are presented as mean (± SEM). Significance levels at $^{*}p < 0.05$ *vs.* Con group and $^{\dagger}p < 0.05$ *vs.* Aged group

correlations between them, while these dilations were slightly observed in the LG-incubated aged rat cells (c). A normal cellular appearance was noted in the control group rat cells (a).

The direct effect of LG on aging-associated increases in $[Na^+]_i$ of ventricular cardiomyocytes seems to be related to the upregulation of SGLT2

As presented in the previous section, our data demonstrated that there were no significant alterations in the I_{CaL} and I_{Na} in the ventricular cardiomyocytes of the aged rats (Fig. 2A, B, respectively). However, we determined significant increases in both sites of I_{NCX} (Fig. 2C) and the basal level of $[Ca^{2+}]_i$ (Fig. 4A). To assess first whether $[Na^+]_i$ can be affected by aging in ventricular cardiomyocytes and then second to examine whether LG has a direct effect on this parameter, we determined the $[Na^+]_i$ in a Na^+-specific fluorescence dye-loaded ventricular cardiomyocytes from the aged rats with or without LG application (100 nM for 3–4-h incubation). As can be seen in Fig. 5A, there was a significant increase

in the basal $[Na^+]_i$ in the aged rat cardiomyocytes, while that increase was slightly but significantly ameliorated by the LG treatment.

Since we previously have shown a significant increase in the protein and mRNA levels of the sodium-glucose co-transporter 2 (SGLT2) in the ventricular cardiomyocytes of aged rats [28], and to test the possible contribution of activated SGLT2 to increased $[Na^+]_i$, we determined the protein level of SGLT2 in the aged rat cardiomyocytes either treated or untreated with LG (100 nM for 3–4-h incubation). As given in Fig. 5B, the significantly increased SGLT2 protein level in the aged rat cardiomyocytes was found to be fully ameliorated in the LG-treated cardiomyocytes.

An examination of a direct LG effect on the cellular glucose regulation of aged rat ventricular cardiomyocytes

In these groups of examinations, we first examined the protein levels of the insulin receptor substrate-1 (IRS1) and the insulin-responsive glucose transporter (GLUT4) in ventricular cardiomyocytes from the aged rats. Compared to those of adults, the IRS1 protein level in the aged cardiomyocytes was significantly decreased (Fig. 6A). The LG treatment of these cells (100 nM for 3–4-h incubation) could significantly attenuate this increase in IRS1 protein level.

As can be seen in Fig. 6B, the protein level of GLUT4 was significantly low in the untreated aged rat cardiomyocytes in comparison to those of adults. The LG treatment of these aged rat cardiomyocytes did not affect this decrease, significantly (Fig. 6B).

The cardioprotective effect of LG is associated with its recovery effect in the activated IRS1-eNOS-PKG pathway

In the last part of these groups of examinations, taking into consideration the previously published data related to the possible direct effect of LG on cardiac remodeling through the activation of the IRS1-eNOS-PKG pathway, we first determined the protein levels of protein kinase G (PKG), a signaling protein in this pathway, in either LG-treated (100 nM for 3–4-h incubation) or untreated groups of the aged rat cardiomyocytes in comparison to those of adults. As can be seen in Fig. 6C, the LG treatment of aged rat cardiomyocytes was able to significantly ameliorate the increased level of PKG when compared to adults.

We, further, examined another signaling molecule, the phosphorylation and protein levels of endothelial nitric oxide synthase (pNOS3 and NOS3, respectively), in aged rat cardiomyocytes. As given in Fig. 6D, the ratio of pNOS3 to NOS3 level is found to be increased in aged rat ventricular cardiomyocytes compared to those of adults. Indeed, both levels of pNOS3 and NOS3 (for reference protein β-actin) were increased significantly in the aged rats' group. The treatment of these cells with LG provided also a significant recovery in this ratio.

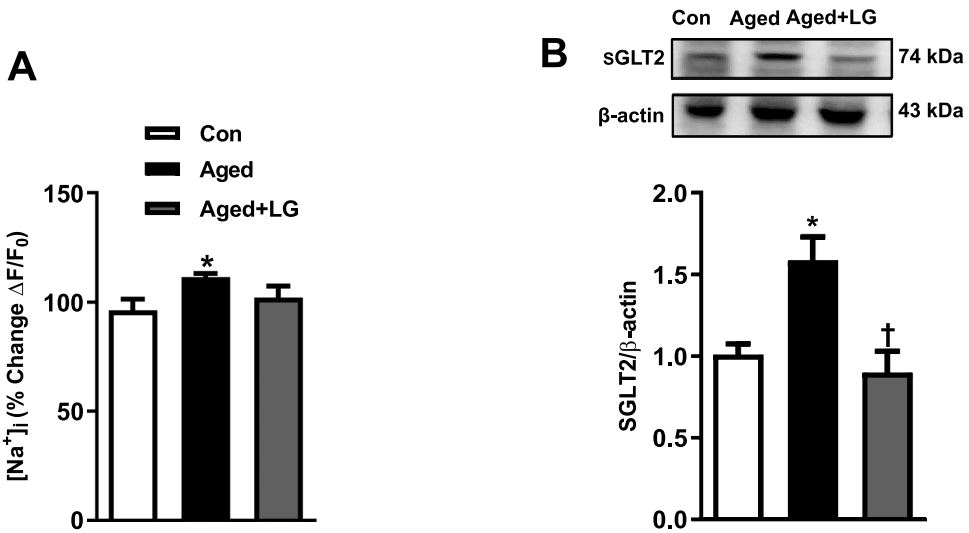

Fig. 5 The direct effect of LG on aging-associated increases in $[Na^+]_i$ of ventricular cardiomyocytes seems to be related to the upregulation of SGLT2. **A** The $[Na^+]_i$ in a Na^+-specific fluorescence dye (SBFI) loaded ventricular cardiomyocytes from rats. The cells are treated with LG (100 nM for 3–4-h incubation). The experimental animal groups are LG-treated aged rats (Aged + LG group), untreated aged rats (Aged group), and adult rats (Con group). **B** The protein level of SGLT2 in the ventricular cardiomyocytes from rats was determined by Western blot analysis. The representative protein bands given in the upper part of the bar graphs and β-actin are used for a reference protein. The data were from at least 25–30 recordings from 15 to 20 cells/group from 5 to 6 rats per group. The bar graphs are presented as mean (±SEM). Significance levels at $^*p < 0.05$ *vs.* Con group and $^\dagger p < 0.05$ *vs.* Aged group

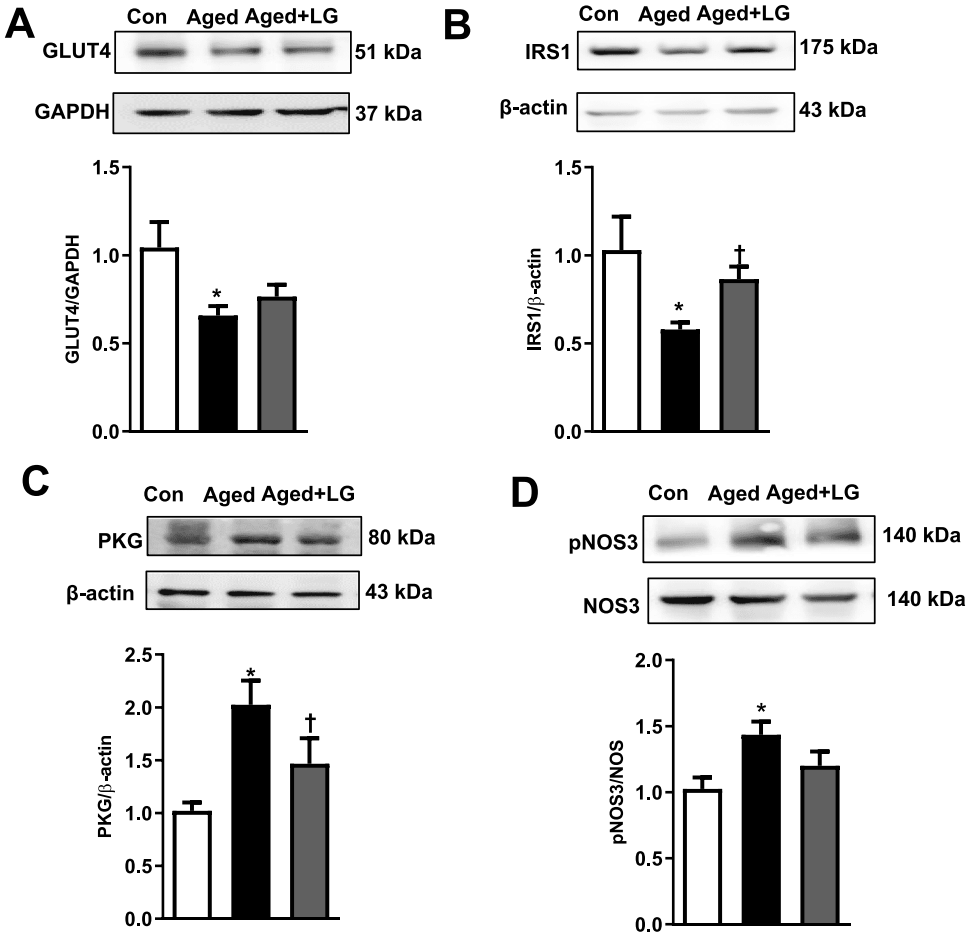

Fig. 6 The examination of a direct LG effect on cellular glucose regulation of aged rat ventricular cardiomyocytes. All Western blot analyses were performed in LG-incubated (100 nM for 4 h) aged rat cardiomyocytes in comparison with either untreated aged cardiomyocytes or controls. **A** The representative Western blot protein bands (upper part) for IRS-1 and their calculated protein levels with respect to the reference protein β-actin (lower part). **B** The representative Western blot protein bands (upper part) for GLUT4 and their calculated protein levels with respect to the reference protein GAPDH (lower part). **C** The representative Western blot protein bands (upper part) for PKG and their calculated protein levels with respect to the reference protein β-actin (lower part). **D** The representative Western blot protein bands (upper part) for pNOS3 and NOS3 and the determined ratio of these proteins calculated with a reference protein β-actin. The bar graphs are representing the mean (±SEM) values of the groups and measurements with double assays in each sample from each group for every Western blot analysis. Significance level at $^{*}p<0.05$ *vs.* Con group and $^{\dagger}p<0.05$ *vs.* Aged group

Discussion

We, here, demonstrated the significant effects of LG treatment on elderly rats in terms of their systemic parameters, as well as at the cellular and subcellular levels in isolated ventricular cardiomyocytes. Our further analysis of whole system parameters (i.e., plasma TOS and TAS levels) and cell-level evaluations (i.e., cellular ROS and RNS levels) treated with LG implies that these observed benefits, at least, are associated with antioxidant-like action. Similar to previous study results, here, we demonstrated for the first time LG treatment-associated recoveries in the blood pressure and electrical activity of the aged rat heart [13, 30]. These observed recoveries were further supported by our findings in isolated ventricular cardiomyocytes from the LG-treated aged rats. Among these findings, there are recoveries in the electrical activities of the cardiomyocytes (i.e., parameters of APs) through recoveries in the depressed I_K and activated I_{NCX}. We also determined significant amelioration in cellular Ca^{2+} dysregulation with in vivo LG treatment of the aged rats. Moreover, our in vitro experimental analysis performed in the ventricular cardiomyocytes, particularly associated with mitochondria, also strongly implied LG-directed cardioprotective effects on the aging heart, through the attenuation of high ROS production. More importantly, our present data, for the first time demonstrated that an in vitro treatment of aged rat cardiomyocytes with LG could prevent the high $[Na^+]_i$, most probably via a full inhibition of activated SGLT2 in these cardiomyocytes. Our further investigation with LG-treated aged cardiomyocytes also demonstrated the

important involvement of the LG effect on the IRS1-eNOS-PKG signaling pathway. In this regard, we have shown significant recoveries in high RNS levels, activated PKG, and pNOS3/NOS3. Under our present data, a possible molecular mechanism of LG action on electrophysiological and biochemical properties of insulin-resistant aged rat cardiomyocytes is given in Fig. 7. A supporting study was presented by Chen et al. performed among rats with heart failure treated with exendin-4. They, in their study, demonstrated that the exendin-4 treatment ameliorated the abnormal remodeling in the heart via affecting the eNOS/cGMP/PKG in addition to its receptor-associated action [8]. Accordingly, our present data with LG application (such as RNS, PKG, and pNOS3/NOS3, under both in vivo and in vitro conditions) can demonstrate that GLP-1R agonism has a cardioprotective action in its affecting different pathways, including the eNOS/cGMP/PKG pathway in the aged cardiomyocytes. Taking into consideration recent clinical and experimental findings, our data, for the first time, provided some important information on the direct cardioprotective effects of GLP-1 agonism in aged rats, through reserving the electrical and ionic properties of ventricular cardiomyocytes, at most, affecting positively the mitochondrial dysfunction, activated SGLT2, and also both ROS and RNS-induced injury in aged ventricular cardiomyocytes.

It is well documented that there are significant changes in intracellular Ca^{2+} regulation in particularly ventricular cardiomyocytes isolated from senescent mammalian hearts, including excess Ca^{2+} loading; changes in responses to either electrical, pharmacological, or both types of stimulations; and marked changes in the balance of oxidative stress and thee antioxidant defense system. Here, we demonstrated a significant cardioprotective effect of LG application on the above changes, defined as remodeling in cells under physiological aging. The systemic changes in the heart during the aging period are also characterized by changes in cardiometabolic parameters, the contribution of impaired redox status, in addition to changes in the organelle dynamics, including mitochondrial dysfunction [21, 29]. Accordingly, there is great interest in the use of new oral glucose-lowering agents such as SGLT2 inhibitors, GLP-1 agonists, and DPP-4 inhibitors in diabetics and nondiabetics with

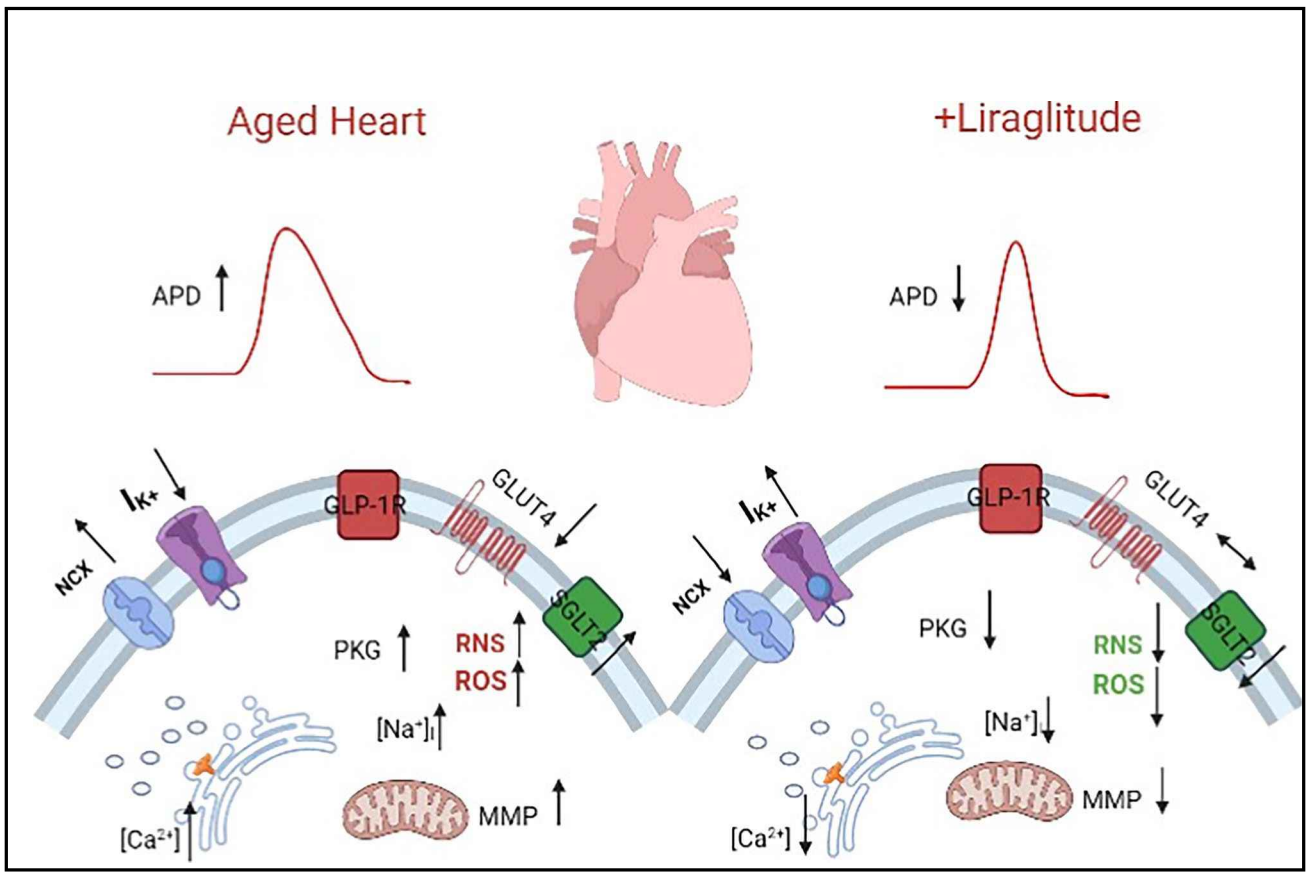

Fig. 7 A possible molecular mechanism of LG effect on electrophysiological and biochemical properties of insulin-resistant aged rat cardiomyocytes. The recoveries in prolonged APDs, depressed IK, increased INCX, increased $[Ca^{2+}]_i$ and $[Na.^{+}]_i$, depressed IRS1, and activated SGLT2, PKG, and p-eNOS (eNOS by LG application seems to be closely associated with recoveries in MMP and productions of ROS and RNS in ventricular cardiomyocytes from aged rats)

insulin resistance [9]. In this regard, although GLP-1 has a glucose-regulatory action via the stimulation of insulin secretion and glucagon suppression in a glucose-dependent manner, it has been also demonstrated that glucose-lowering agents can reduce the risk of major CVDs via affecting systematically and/or organ/cell-targeting manner [11, 26, 29]. For instance, GLP-1 can acutely increases heart rate, and this effect of GLP-1 on nodal tissue appears to be indirect, mediated via the increased activity of the sympathetic nervous system [26]. The last statement, indeed, has supported the hypothesis related to its direct effect on heart function beyond its glucose-lowering action.

However, despite the evidence of the role of GLP-1 in the cardiovascular system, the direct effects of GLP-1R agonists on the electrical properties of the myocardium (in vivo) and ventricular cardiomyocytes (in vitro) remain unclear. Accordingly, there are some experimental studies supporting our present study in the literature. For instance, the authors performed experiments in rats with a GLP-1R agonist exendin-4 (4 weeks) treatment and determined its beneficial effect on cardiac ventricular excitability and reduction of ventricular arrhythmic potential through its affecting cellular Ca^{2+} dysregulation [1]. Also, another supporting study was performed with GLP-1 to test whether it has a direct cardiac effect and to identify the underlying mechanisms of its effect in HL-1 cultured cardiomyocytes. In that study, it was demonstrated that the GLP-1 (10 nM) application was able to significantly increase the transient changes of $[Ca^{2+}]_i$ and SR Ca^{2+} level via a recovery in hyperphosphorylated RyR2 and total phospholamban [15]. Their data further imply the modulatory effect of GLP-1 on cell arrhythmogenesis through the modulation of Ca^{2+} handling proteins.

Our in vitro studies with GLP-1 agonism in aged rat cardiomyocytes strongly support its direct cardioprotective effect besides its receptor-associated action. In this regard, the direct effect of LG on the aging-associated upregulation of SGLT2 and an increase in $[Na^+]_i$ also strongly support our hypothesis in terms of a direct cardiac targeting action of GLP-1 agonism in the aged rat heart. Correspondingly, clinical studies have supported our present results by presenting the important impact of the SGLT2 inhibitor addition on GLP-1 agonist therapy in people with type 2 diabetes [9]. Therefore, our present data include fully new documents on this topic and provide important new therapeutic approaches to provide a healthy heart function in aged individuals. Consequently, most in vitro studies with GLP-1R agonists, being parallel to in vivo studies and clinical outcomes, strongly suggest that GLP-1 agonism can target the heart and may provide cardioprotection under any pathological stimuli besides diabetes.

Acknowledgements The authors thank Drs. S. Degirmenci and D. Billur for their technical supports.

Author contribution The authors declare that all data were generated in-house and that no paper mill was used. Belma Turan conceived of the study and wrote the manuscript and Aysegul Durak performed the majority of the experiments.

Funding This work was supported by Grants to B.T. (No. SBAG119S661) from The Scientific and Technological Research Council of Turkey.

Data availability Data are available from the authors upon request.

Declarations

Ethics approval Our study followed the guidelines for the care and use of animals.

Informed consent All authors involved in the study accept the contents of the manuscript and consent to the submission of the work.

Conflict of interest The authors declare no competing interests.

References

1. Ang R et al (2018) Modulation of cardiac ventricular excitability by GLP-1 (glucagon-like peptide-1). Circ Arrhythm Electrophysiol 11(10):e006740
2. Bai X-J et al (2021) Glucagon-like peptide-1 analog liraglutide attenuates pressure-overload induced cardiac hypertrophy and apoptosis through activating ATP sensitive potassium channels. Cardiovasc Drugs Ther 35(1):87–101
3. Bhashyam S, Parikh P, Bolukoglu H, Shannon AH, Porter JH, Shen Y-T, Shannon RP (2007) Aging is associated with myocardial insulin resistance and mitochondrial dysfunction. Am J Physiol Heart Circ Physiol 293(5):H3063–H3071
4. Billur D et al (2016) Interplay between cytosolic free Zn(2+) and mitochondrion morphological changes in rat ventricular cardiomyocytes. Biol Trace Elem Res 174(1):177–188
5. Boudina S (2013) Cardiac aging and insulin resistance: could insulin/insulin-like growth factor (IGF) signaling be used as a therapeutic target? Curr Pharm Des 19(32):5684–5694
6. Brand CL et al (2009) Synergistic effect of the human GLP-1 analogue liraglutide and a dual PPARalpha/gamma agonist on glycaemic control in Zucker diabetic fatty rats. Diabetes Obes Metab 11(8):795–803
7. Chason KD et al (2018) Age-associated changes in the respiratory epithelial response to influenza infection. J Gerontol A Biol Sci Med Sci 73(12):1643–1650
8. Chen J et al (2017) Exendin-4 inhibits structural remodeling and improves Ca(2+) homeostasis in rats with heart failure via the GLP-1 receptor through the eNOS/cGMP/PKG pathway. Peptides 90:69–77
9. Curtis L et al (2016) Addition of SGLT2 inhibitor to GLP-1 agonist therapy in people with type 2 diabetes and suboptimal glycaemic control. Practical Diabetes 33(4):129–132
10. Durak A et al (2021) GLP-1 receptor agonist treatment of high-carbohydrate intake-induced metabolic syndrome provides pleiotropic effects on cardiac dysfunction through alleviations in electrical and intracellular Ca(2+) abnormalities and mitochondrial dysfunction. Clin Exp Pharmacol Physiol
11. Durak A et al (2018) A SGLT2 inhibitor dapagliflozin suppresses prolonged ventricular-repolarization through augmentation of

mitochondrial function in insulin-resistant metabolic syndrome rats. Cardiovasc Diabetol 17(1):144
12. Gaspari T et al (2011) A GLP-1 receptor agonist liraglutide inhibits endothelial cell dysfunction and vascular adhesion molecule expression in an ApoE-/- mouse model. Diab Vasc Dis Res 8(2):117–124
13. Hacker TA et al (2006) Age-related changes in cardiac structure and function in Fischer 344× Brown Norway hybrid rats. Am J Physiol Heart Circ Physiol 290(1):H304–H311
14. Han S et al (2008) Dapagliflozin, a selective SGLT2 inhibitor, improves glucose homeostasis in normal and diabetic rats. Diabetes 57(6):1723–1729
15. Huang JH et al (2016) Glucagon-like peptide-1 regulates calcium homeostasis and electrophysiological activities of HL-1 cardiomyocytes. Peptides 78:91–98
16. Knudsen LB (2010) Liraglutide: the therapeutic promise from animal models. Int J Clin Pract Suppl 167:4–11
17. Kobara M, Toba H, Nakata T (2022) A glucagon-like peptide 1 analogue protects mitochondria and attenuates hypoxia-reoxygenation injury in cultured cardiomyocytes. J Cardiovasc Pharmacol 79(4):568–576
18. Lakatta EG, Sollott SJ, Pepe S (2001) The old heart: operating on the edge. Novartis Found Symp 235:172–96 (**discussion 196-201, 217-20**)
19. Langlois A et al (2016) In vitro and in vivo investigation of the angiogenic effects of liraglutide during islet transplantation. PLoS ONE 11(3):e0147068
20. Larsen PJ et al (2008) Combination of the insulin sensitizer, pioglitazone, and the long-acting GLP-1 human analog, liraglutide, exerts potent synergistic glucose-lowering efficacy in severely diabetic ZDF rats. Diabetes Obes Metab 10(4):301–311
21. Lesnefsky EJ, Chen Q, Hoppel CL (2016) Mitochondrial metabolism in aging heart. Circ Res 118(10):1593–1611
22. Ma X, Liu Z, Ilyas I, Little PJ, Kamato D, Sahebka A, Chen Z, Luo S, Zheng X, Weng J, Xu S (2021) GLP-1 receptor agonists (GLP-1RAs): cardiovascular actions and therapeutic potential. Int J Biol Sci 17(8):2050–2068
23. Matthews DR et al (1985) Homeostasis model assessment: insulin resistance and β-cell function from fasting plasma glucose and insulin concentrations in man. Diabetologia 28(7):412–419
24. Morales PE et al (2014) GLP-1 promotes mitochondrial metabolism in vascular smooth muscle cells by enhancing endoplasmic reticulum-mitochondria coupling. Biochem Biophys Res Commun 446(1):410–416
25. Muller TD et al (2019) Glucagon-like peptide 1 (GLP-1). Mol Metab 30:72–130
26. Noyan-Ashraf MH et al (2009) GLP-1R agonist liraglutide activates cytoprotective pathways and improves outcomes after experimental myocardial infarction in mice. Diabetes 58(4):975–983
27. Okatan EN, Durak AT, Turan B (2016) Electrophysiological basis of metabolic-syndrome-induced cardiac dysfunction. Can J Physiol Pharmacol 94(10):1064–1073
28. Olgar Y et al (2020) Ageing-associated increase in SGLT2 disrupts mitochondrial/sarcoplasmic reticulum Ca(2+) homeostasis and promotes cardiac dysfunction. J Cell Mol Med 24(15):8567–8578
29. Olgar Y et al (2020) MitoTEMPO provides an antiarrhythmic effect in aged-rats through attenuation of mitochondrial reactive oxygen species. Exp Gerontol 136:110961
30. Olgar Y et al (2022) Insulin acts as an atypical KCNQ1/KCNE1-current activator and reverses long QT in insulin-resistant aged rats by accelerating the ventricular action potential repolarization through affecting the β3-adrenergic receptor signaling pathway. J Cell Physiol 237(2):1353–1371
31. Pataky MW, Young WF, Nair KS (2021) Hormonal and metabolic changes of aging and the influence of lifestyle modifications. Mayo Clin Proc 96(3):788–814
32. Patorno E et al (2021) Comparative effectiveness and safety of sodium-glucose cotransporter 2 inhibitors versus glucagon-like peptide 1 receptor agonists in older adults. Diabetes Care 44(3):826–835
33. Refaie MR et al (2006) Aging is an inevitable risk factor for insulin resistance. J Taibah Univ Med Sci 1(1):30–41
34. Shpilberg Y et al (2012) A rodent model of rapid-onset diabetes induced by glucocorticoids and high-fat feeding. Dis Model Mech 5(5):671–680
35. Singh Y et al (2013) A study of insulin resistance by HOMA-IR and its cut-off value to identify metabolic syndrome in urban Indian adolescents. J Clin Res Pediatr Endocrinol 5(4):245
36. Zinman B et al (2015) Empagliflozin, cardiovascular outcomes, and mortality in type 2 diabetes. N Engl J Med 373(22):2117–2128